

## Chute Flows

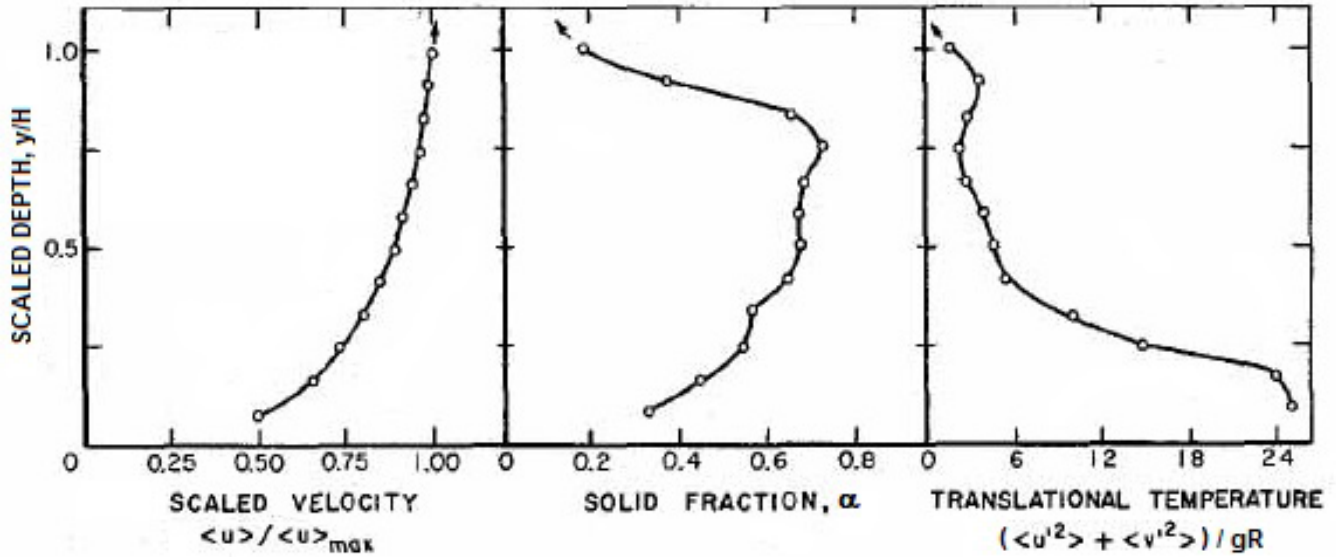


Figure 1: Typical profiles of velocity,  $u$ , solid fraction,  $\alpha$ , and granular temperature in a chute flow. From the simulations of Campbell and Brennen (1985b).

Typical profiles of velocity,  $u$ , solid fraction,  $\alpha$ , and granular temperature in a rapid chute flow are shown in Figure 1 where  $y$  is the elevation above the chute bed and  $H$  is the depth of the layer (for further details see section (Npm)). Unlike a liquid the granular material exhibits slip at the wall and that slip depends on the characteristics of the chute surface (see Ahn *et al.* 1987). Because of the high shear rate and granular temperature near the chute bed, the solid fraction,  $\alpha$ , is substantially smaller in that region. Moreover, near the surface of the granular material there is a surface layer in which the material is fluidized leading to a low solid fraction.

It is convenient to define two Froude numbers  $Fr$  and  $Fr^*$  for these granular chute flows:

$$Fr = \frac{\dot{m}}{\rho_S \alpha b H (gH)^{1/2}} \quad Fr^* = \frac{Fr}{(\cos \theta)^{1/2}} \quad (\text{Npq1})$$

where  $\dot{m}$  is the mass flow rate,  $\rho_S$  is the material density and  $b$  and  $\theta$  are the breadth and inclination of the chute. If  $\alpha$  were the cross-sectionally averaged solids fraction at a particular point, then  $Fr$  would represent the average material velocity divided by  $(gH)^{1/2}$ . However, in contrast to the open channel flow of a liquid, the average solids fraction or density at a particular location cannot be assumed to be known or uniform. In concert with the semantics of the open channel flow of liquid, flows with  $Fr^* < 1$  or  $Fr^* > 1$  will be referred to as subcritical or supercritical respectively.

As with a liquid flow, the state of the granular flow in a chute will be determined by the conditions at inlet to and discharge from the chute. Normally a flow restriction at inlet results in a supercritical flow that, without downstream restriction, persists all the way to the discharge. However, the introduction of a discharge restriction would then cause the formation of a hydraulic jump that propagates upstream with

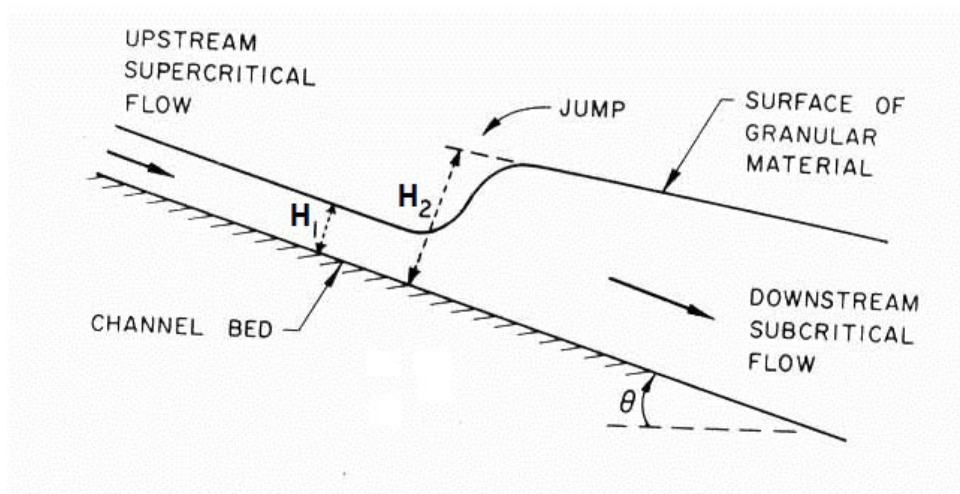


Figure 2: Notation for a granular flow hydraulic jump in an inclined chute. From Brennen *et al.* (1983).

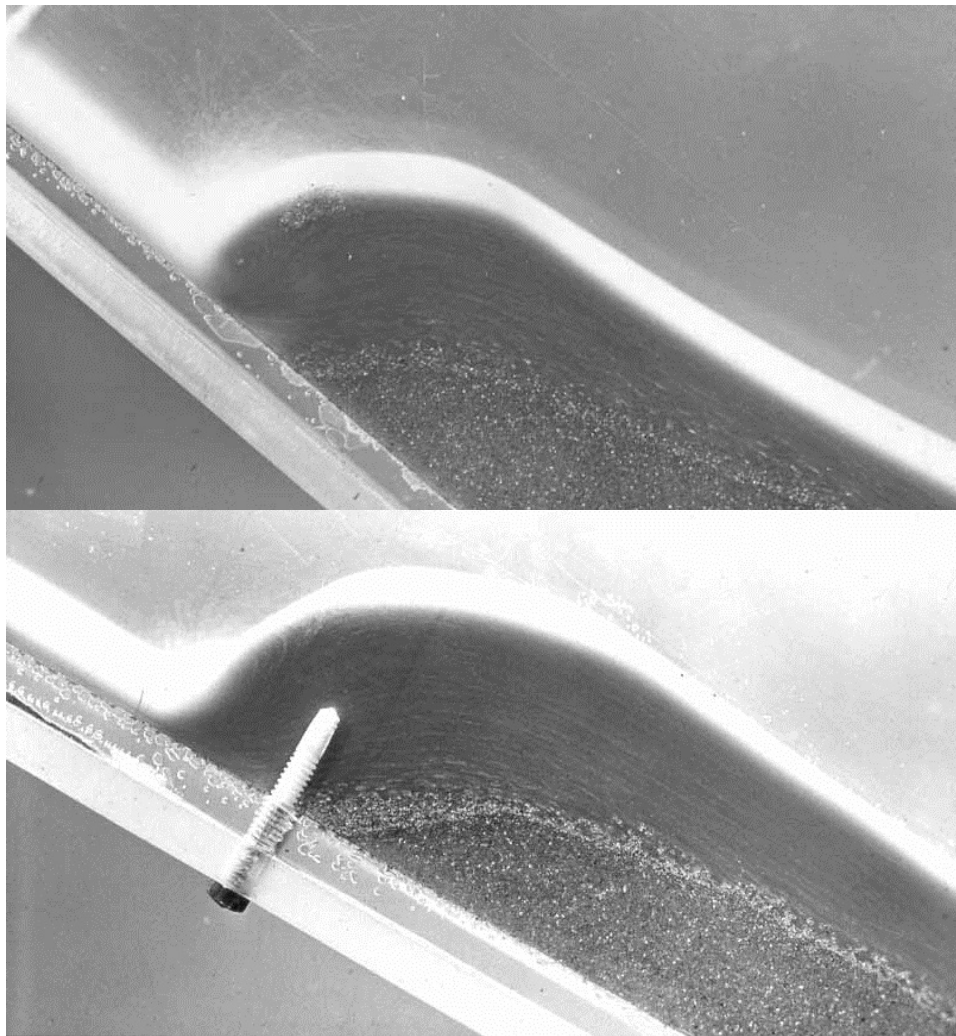


Figure 3: Examples of steady granular flow hydraulic jumps in an inclined chute. From Brennen *et al.* (1983).

subcritical flow downstream of the jump. If the jump propagates all the way to the inlet, the flow will slow or halt. In other circumstances, the jump may come to a halt at some location location between the inlet

and discharge.

Figure 2 depicts a jump at rest with upstream and downstream conditions denoted by the subscripts 1 and 2. Figure 3 contains two photographs of stationary granular hydraulic jumps. The flow upstream is quite thin and barely visible. The flow immediately downstream of the jump contains an obvious lateral vortex; further downstream the layer contains a flowing layer riding over a stagnant layer.

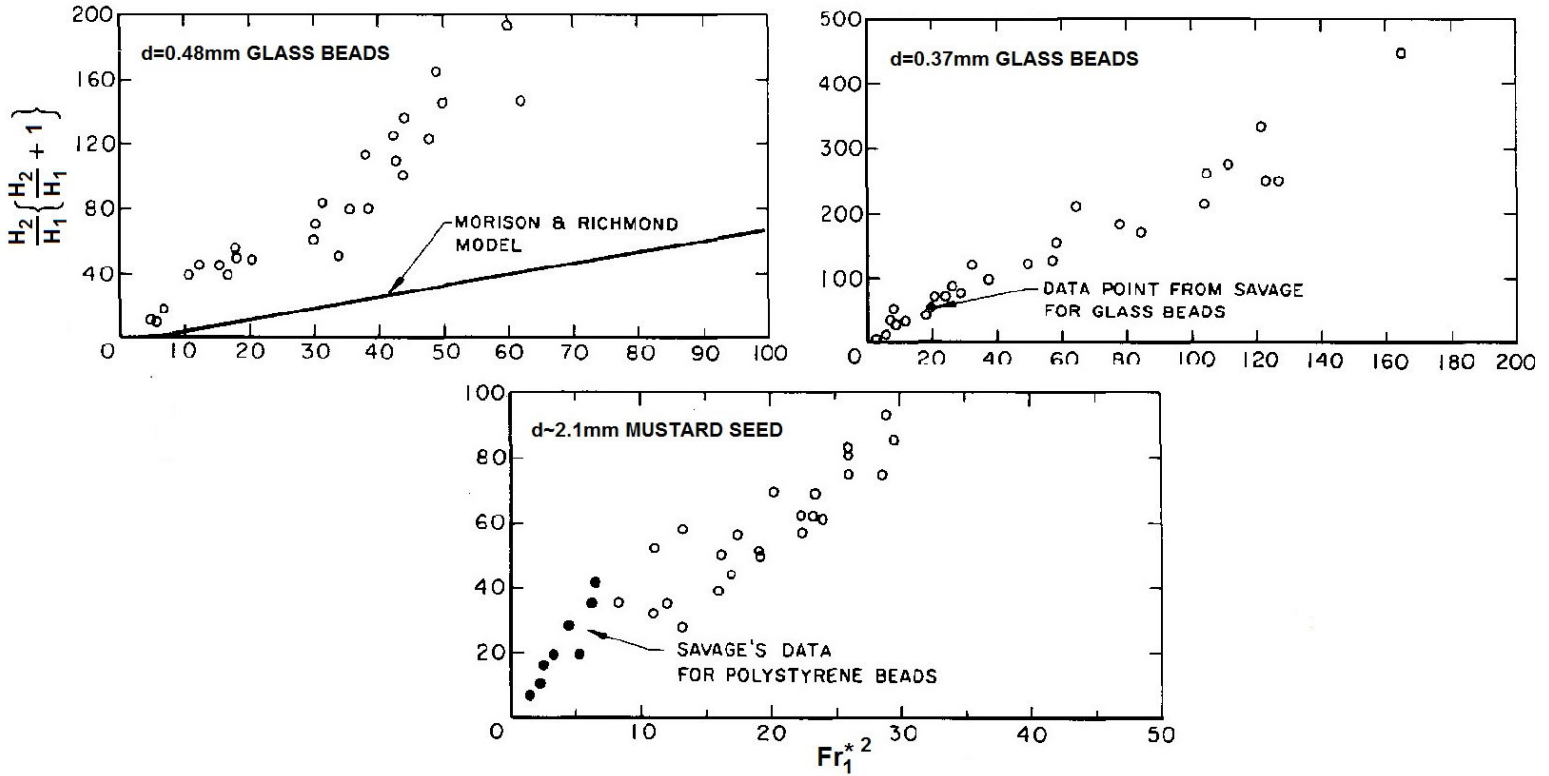


Figure 4: Experimental values of  $(H_2/H_1)[(H_2/H_1) + 1]$  plotted versus  $(Fr_1^*)^2$  for granular hydraulic jumps of three granular materials and a wide range of flow rates. Adapted from Brennen *et al.* (1983).

In open channel flow of either a liquid or a granular material, the ratio  $H_2/H_1$  is determined by the laws of mass conservation and momentum (see section (Bpc) for details). In general, these lead to the following approximate relation between  $H_2/H_1$  and  $Fr_1^*$ :

$$2C(Fr_1^*)^2 = \left( \frac{H_2}{H_1} \right) \left[ \frac{H_2}{H_1} + 1 \right] \quad (\text{Npq3})$$

where  $C$  is a dimensionless parameter that depends on the shapes of the velocity, solid fraction and pressure profiles that, for present purposes, are assumed to have the same shape upstream and downstream of the jump (see Ahn *et al.* 1987). It is therefore appropriate to plot experimental measurements of  $(H_2/H_1)[(H_2/H_1) + 1]$  against  $(Fr_1^*)^2$  in order to assess actual values of the profile parameter,  $C$ . Figure 4 presents data from Brennen *et al.* (1983) for a wide range of flow rates (different  $\theta$  and  $H_1$ ) and for two sizes of glass beads and mustard seed. Evidently this data conforms quite closely to equations (Npq3) with values of  $C$  of approximately 1.5 for all particles and flow conditions.